EurJIC
European Journal of Inorganic Chemistry

A Journal of ChemPubSoc Europe

Accepted Article

Title: Self-assembled palladium and platinum coordination cages: Photophysical studies and anticancer activity

Authors: Felix Kaiser; Andrea Schmidt; Wolfgang Heydenreuter; Philipp Johannes Altmann; Angela Casini; Stephan A. Sieber; Fritz Elmar Kühn

To be cited as: Eur. J. Inorg. Chem. 10.1002/ejic.201600811

Link to VoR: http://dx.doi.org/10.1002/ejic.201600811

WILEY-VCH

Self-assembled palladium and platinum coordination cages: Photophysical studies and anticancer activity

Felix Kaiser,[a] Andrea Schmidt,[a] Wolfgang Heydenreuter,[b] Philipp J. Altmann,[a] Angela Casini,[c] Stephan A. Sieber[b] and Fritz E. Kühn[a]*

Abstract: Self-assembled coordination cages are interesting as drug delivery systems. Therefore, the synthesis of new M_2L_4 (M = Pd, Pt) molecular cages, derived from highly fluorescent, rigid polyaromatic ligands is reported and the first Pt_2L_4 cage with a ligand consisting of three pyridine moieties is described. Photophysical properties were examined showing high quantum yields Φ of up to 48% for the methoxy-functionalized ligands. Coordination of the ligands to palladium and platinum ions reduces the metallocages' fluorescence, however. The host-guest chemistry of the palladium cages with cisplatin is investigated confirming the encapsulation. The cages encapsulating cisplatin show a significantly increased cytotoxicity towards A549 (human lung adenocarcinoma) cells compared to cisplatin, and thus appear to be promising delivery vectors for the anticancer drug cisplatin.

Introduction

Almost two decades have passed, since McMorran and Steel reported the first Pd_2L_4 molecular cage, capable of enclosing a hexafluorophosphate counterion.[1] Since then increasing interest on M_2L_4 complexes with inner cavities has emerged, as they are readily accessible through self-assembly by simply mixing bidentate ligands and metal precursors. The assemblies rely largely on coordinative interactions of Pd^{2+} and pyridine moieties,[2] although some examples with different metal ions, such as Pt^{2+},[3] Co^{2+},[4] Cu^{2+},[5] and Zn^{2+} are known.[3a, 4e] So far only a few fluorescent M_2L_4 cages were obtained using ligands with extensive π-systems or attached fluorophores,[3a, 6] although highly fluorescent metallocages would be very interesting for biological imaging in cells by fluorescence microscopy. Aside from fluorescence, the encapsulation of (counter)ions has been reported.[4a-d, 5a, 7] Moreover, supramolecular coordination complexes are also capable to encapsulate metal compounds[2b, 6b, 8] (e.g. cisplatin) and some of them have been tested concerning their cytotoxicity for cancer cells.[8a-e, 9] Cisplatin is one of the most widely applied anticancer agent against ovarian, bladder and testicular cancer to name just a few.[10] However, its effectiveness is accompanied by severe side effects, thus limiting the applicable dose.[10b] The necessity to reduce side effects and toxicity of cisplatin and its derivatives has gained growing appreciation in current research. One possibility is to utilize the so called EPR (= enhanced permeability and retention) effect, which was discovered in 1986 by Maeda and Matsamura.[11] Until now a plethora of vectors for cisplatin has been examined, e. g. liposomes,[12] nanoparticles,[13] macrocycles,[14] and as already mentioned above, also metallocages.[8c, g] Recently, our group evaluated palladium cage compounds as drug delivery systems for cisplatin *in vitro* in cancer cells and *ex vivo* in healthy rat liver tissue.[6e, 8a] Goal of this research is to ensure a safe transport of the active molecules selectively to the target entity. Solubility, toxicity and size of the transporter are of high importance in this context. Based on recent results, in this work the synthesis and characterization of new M_2L_4 molecular cages with enhanced solubility are described. The photophysical properties of the metallocages were investigated, in order to examine the possibility of uptake studies in cells. The incorporation of electron-donating methoxy groups in the ligand framework could potentially increase the photoluminescence of the ligands, thus enhancing the emissive properties of the metallocages. Moreover, the host guest relationship with cisplatin is examined for the palladium cages and the cytotoxicity of the cages and their cisplatin inclusion compounds towards human cancer cells is examined *in vitro*.

Results and discussion

Rigid bis-monodentate pyridyl ligands **2** and **3**, bearing functionalizable methoxy moieties were obtained *via* divergent synthesis based on Sonogashira cross coupling reactions (Scheme 1). Compound **1** was synthesized in a two-step literature procedure.[15] A Sonogashira reaction of **1** with 3,5-dibromo aniline yielded **2** as a pale yellow solid after flash column chromatography. Likewise, reaction of **1** with 2,6-dibromo pyridine gave ligand **3** as a yellow solid after flash column chromatography. The methoxy-functionalization was supposed to have increased effects on the solubilty and fluorescence properties. Compounds **2** and **3** were characterized by ^1H, ^{13}C, DOSY NMR, ESI HRMS and IR spectroscopy.

[a] F. Kaiser, A. Schmidt, P. J. Altmann, Prof. Dr. F. E. Kühn
Catalysis Research Center and Department of Chemistry, Technische Universität München, Lichtenbergstr. 4, 85747 Garching bei München, Germany.
E-Mail: fritz.kuehn@ch.tum.de
[b] W. Heydenreuter, Prof. Dr. S. A. Sieber
Center for Integrated Protein Science Munich (CIPS^M), Department of Chemistry, Technische Universität München, Lichtenbergstraße 4, 85747 Garching bei München, Germany.
E-Mail: stephan.sieber@mytum.de
[c] Prof. Dr. A. Casini
School of Chemistry, Cardiff University, Park Place, CF103AT Cardiff, UK.
E-Mail: CasiniA@cardiff.ac.uk

Supporting information for this article is available on the WWW under http://dx.doi.org/xxxxxx..

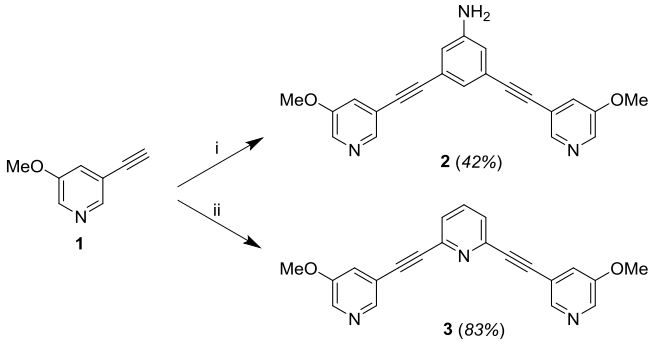

Scheme 1. Preparation of ligands **2** and **3**. Reagents and conditions: i) 3,5-dibromo aniline, $[PdCl_2(PPh_3)_2]$, CuI, rfx., 3 d, (NEt_3); ii) 2,6-dibromo pyridine, $[PdCl_2(PPh_3)_2]$, CuI, rfx., 3 d, (NEt_3).

Isostructural M_2L_4 (M = Pd, Pt) cages $\mathbf{2^{Pd}}$, $\mathbf{3^{Pd}}$ and $\mathbf{3^{Pt}}$ were obtained through self-assembly of the ligands **2** and **3** with $[Pd(NCCH_3)_4](BF_4)_2$ or $[Pt(NCCH_3)_2Cl_2]$ and $AgClO_4$, respectively (Scheme 2).

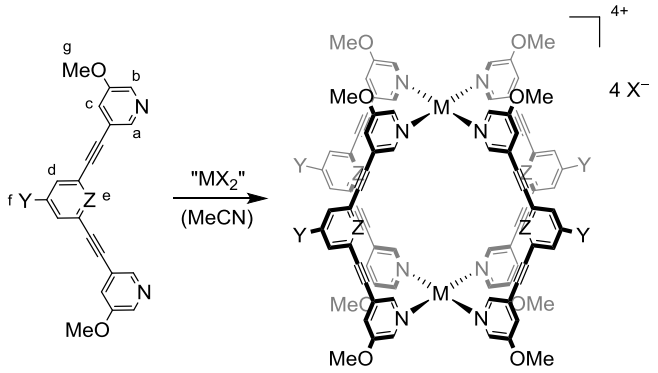

2: Y = NH_2; Z = CH
3: Y = H; Z = N

$\mathbf{2^{Pd}}$: $M^{2+} = Pd^{2+}$; $X^- = BF_4^-$
$\mathbf{3^{Pd}}$: $M^{2+} = Pd^{2+}$; $X^- = BF_4^-$
$\mathbf{3^{Pt}}$: $M^{2+} = Pt^{2+}$; $X^- = ClO_4^-$

Scheme 2. Synthesis of M_2L_4 complexes $\mathbf{2^{Pd}}$, $\mathbf{3^{Pd}}$ and $\mathbf{3^{Pt}}$ *via* self-assembly in acetonitrile. Reagents and conditions: $\mathbf{2^{Pd}}$ and $\mathbf{3^{Pd}}$: $[Pd(NCCH_3)_4](BF_4)_2$, rfx., 1 h; $\mathbf{3^{Pt}}$: $[Pt(NCCH_3)_2Cl_2]$, $AgClO_4$, rfx., 2 d.

The cages were prepared from a suspension of stoichiometric amounts of the starting materials in acetonitrile by heating to reflux for one hour (Pd) or two days (Pt). For the platinum cage $\mathbf{3^{Pt}}$ a purification step *via* column chromatography was necessary.

Cage formation was validated by ^{1}H, DOSY NMR, ESI HRMS, and X-ray structure analysis. In ^{1}H NMR spectra, significant shifts are observed, when comparing the cages and the corresponding free ligands (Figure 1 and Figure 2).

As expected, upon coordination the whole signal sets are shifted downfield for each complex, especially the signals of H_a and H_b. These protons, located in *ortho* position to the coordinating pyridine nitrogen, receive the largest electron withdrawing influence of the metal cations ($\Delta\delta$= 0.47 ppm – 0.59 ppm). Diffusion-ordered NMR spectroscopy (DOSY) gives additional evidence for the formation of M_2L_4 cages.

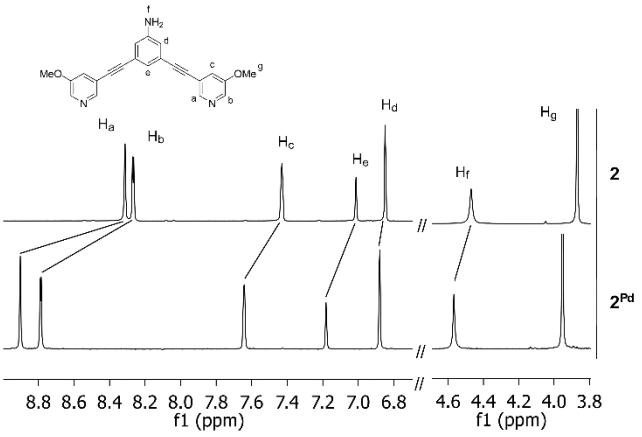

Figure 1. ^{1}H NMR spectra (CD_3CN) of **2** and the corresponding molecular cage $\mathbf{2^{Pd}}$.

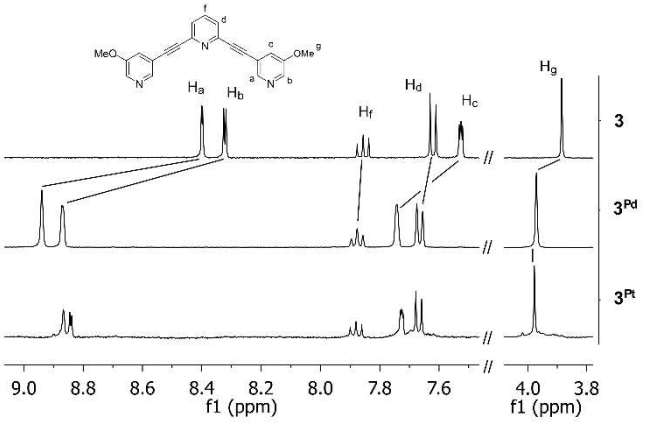

Figure 2. ^{1}H NMR spectra (CD_3CN) of **3** and the cages $\mathbf{3^{Pd}}$ as well as $\mathbf{3^{Pt}}$.

All proton signals of both ligands **2** and **3**, and of the complexes $\mathbf{2^{Pd}}$, $\mathbf{3^{Pd}}$, and $\mathbf{3^{Pt}}$ show the same diffusion coefficient (*D*).

The ratio D_{ligand} to $D_{complex}$ is approximately 2:1, which is due to the presence of larger cage molecules in solution. Using the Einstein-Stokes correlation,[16] the Stokes radii r_0 were calculated for each cage compound. The values are given in Table 1.

Table 1. Diffusion coefficients (*D*) of ligands and M_2L_4 cage complexes in acetonitrile and calculated Stokes radii (r_0).

Component	D (10^{-10} $m^2 \cdot s^{-1}$)	r_0 (Å)
2	10.7	--
$\mathbf{2^{Pd}}$	5.33	11.47
3	12.2	--
$\mathbf{3^{Pd}}$	5.58	10.96
$\mathbf{3^{Pt}}$	5.60	10.92

Electrospray ionization high-resolution mass spectra (ESI HRMS) provide additional support for the formation of the cage complexes. For every cage the signals for the tetra-cationic unit $[M_2L_4]^{4+}$ (M^{2+} = Pd^{2+}, Pt^{2+}; L = **2**, **3**) and its association with one or two counterions. $[M_2L_4](X)_n^{(4-n)+}$ (X^- = BF_4^-, ClO_4^-) are clearly observable (Figure 3, SI). The isotopic distributions fit calculated values, which are exemplarily depicted in Figure 4 for the fragment $[Pt_2\mathbf{3}_4]^{4+}$ in $\mathbf{3^{Pt}}$.

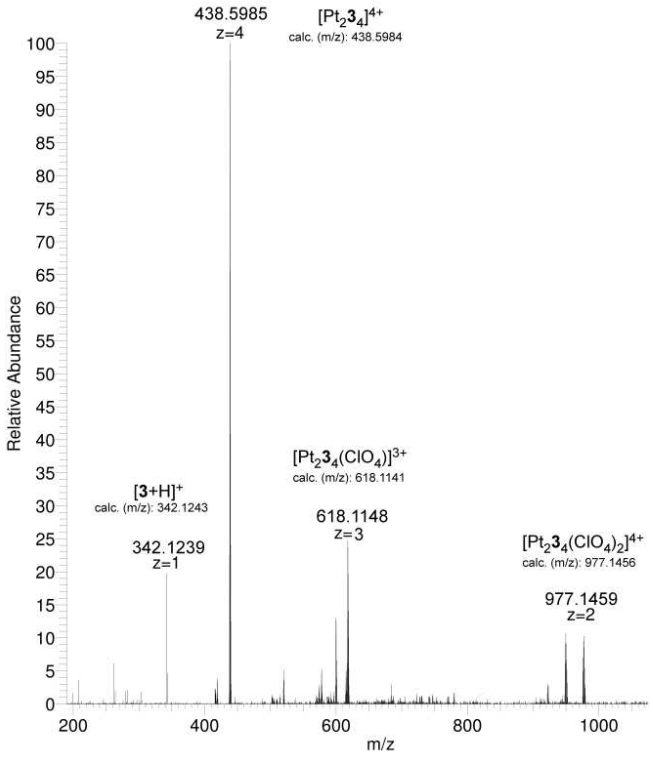

Figure 3. ESI HRMS spectrum cutout of $\mathbf{3}^{Pt}$ with the signals for $[\mathbf{3}+H]^+$ (342.1239), $[Pt_2\mathbf{3}_4]^{4+}$ (438.5985), $[Pt_2\mathbf{3}_4](ClO_4)^{3+}$ (618.1148) and $[Pt_2\mathbf{3}_4](ClO_4)_2^{2+}$ (977.1459).

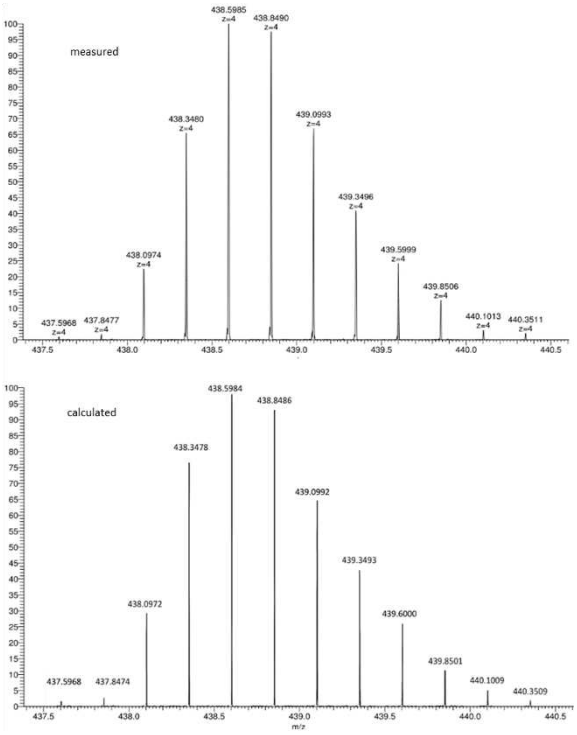

Figure 4. ESI HRMS spectrum cutout of $\mathbf{3}^{Pt}$ with the signals that represent the isotopic distribution of fragment $[Pt_2\mathbf{3}_4]^{4+}$ (top) and the respective calculated spectrum (bottom).

X-ray single crystal structure analysis reveals the formation of paddle wheel shaped coordination cages. Single crystals suitable for single crystal X-ray diffraction were grown by vapor diffusion of diethyl ether into an acetonitrile solution of $\mathbf{2}^{Pd}$ and likewise a solution of $\mathbf{3}^{Pd}$ in acetone over several days.
Cage compound $\mathbf{2}^{Pd}$ crystallizes in the triclinic space group $P\bar{1}$ with the inversion center located centrally inside the cavity (Figure 5).

Each Pd^{II} ion is coordinated in a square-planar fashion by pyridyl moieties of four molecules **2** (angles N–Pd–N between 88.6(1)° and 90.8(2)°), resulting in a lantern-shaped cage with a central cavity. The latter is stocked with disordered solvent molecules, not with counterions. The anions are disordered and located outside the cage, half of them at the apical position of Pd. These observations are in accordance to previously reported results,[8g] although numerous examples of M_2L_4 cage compounds with encapsulated counterions exist in literature as well.[1, 6a, 7a, 17] The cage diameter, calculated between two opposing methoxy-moieties is ≈ 22.6 Å (averaged distances between outer hydrogen atoms). This fits the value calculated from diffusion coefficients (≈ 22.9 Å) well (Table 1). The Pd···Pd distance is 12.0 Å, diagonally opposing central carbon atoms display an averaged distance of 10.5 Å.

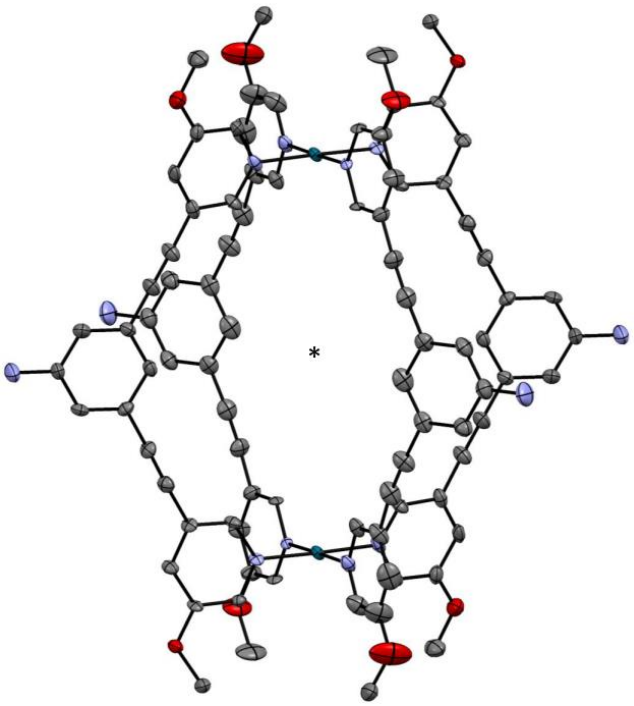

Figure 5. Molecular structure of $\mathbf{2}^{Pd}$. H, co-crystallized solvent and counterions omitted for clarity. Ellipsoids are shown at 50% probability. Element colors: C – grey, N – blue, O – red, Pd – turquoise.

Cage $\mathbf{3}^{Pd}$ also crystallizes in the triclinic space group $P\bar{1}$ with an inversion center located centrally inside the cage (Figure 6). The Pd^{II} ions are again coordinated in a square-planar fashion to one pyridyl moiety of four ligand molecules **3**. The resulting lantern-shaped cage compound exhibits a central cavity that is occupied by two non-disordered acetone molecules. The respective carbonyl oxygen atoms are pointing to the metal ions with a distance of Pd···O of 3.3 Å. The methyl groups are orientated towards the ligands' central pyridine N-atoms with an averaged distance C···N of 3.6 Å. As in $\mathbf{2}^{Pd}$, the BF_4^- counterions are located outside the cage, half of them at the apical position of

Pd^{II}. The cage diameter calculated between two opposing methoxy-moieties is ≈ 22.4 Å (averaged distances between outer hydrogen atoms), which correlates well with the value

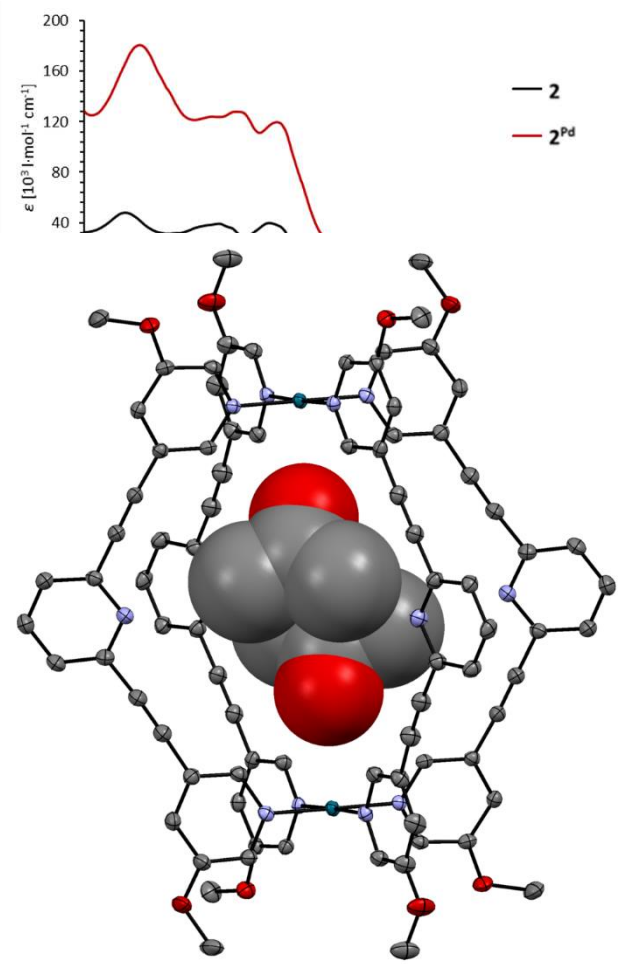

calculated from diffusion coefficients (≈ 21.9 Å, Table 1). The distance between the two Pd atoms is 11.6 Å, diagonally opposing central pyridine N display an averaged distance of 10.9 Å.

Figure 6. Molecular structure of $\mathbf{3}^{Pd}$. Thermal ellipsoids are shown at a 50% probability level. Side view, drawn with two encapsulated acetone molecules (spacefilling representation at 100% of van-der-Waals radii, visualizing the steric demand inside the cage; H and counter ions omitted for clarity. Element colors: C – grey, N – blue, O – red, Pd – turquoise).

Complexes $\mathbf{2}^{Pd}$, $\mathbf{3}^{Pd}$ and $\mathbf{3}^{Pt}$ are soluble in polar solvents like DMSO, DMF, acetonitrile and acetone but insoluble in chloroform, dichloromethane, pentanes or diethyl ether. They are stable in solid state and in solution for weeks. Compound $\mathbf{3}^{Pt}$ is slightly sensitive to oxygen and thus has to be stored under an argon atmosphere.

The ligands' and cages' photophysical properties show a striking dependence on the coordination of metal ions, especially concerning photoluminescence. The absorption spectra of ligand **2** and its corresponding cage are depicted in Figure 7. Ligand **2** displays its strongest absorption bands between 210 and 320 nm and a weaker band is located between 330 and 370 nm. The absorption maximum is observed at 223 nm, with an extinction coefficient ε_{223} (**2**) = 47700 $l \cdot mol^{-1} \cdot cm^{-1}$. Upon coordination to Pd^{II} a bathochromic shift of 9 nm is observed and absorption increases by 3.78 (ε_{232} ($\mathbf{2}^{Pd}$) = 180500 $l \cdot mol^{-1} \cdot cm^{-1}$), only differing by 5% from the estimated quadrupling with respect to the four molecules **2** per complex $\mathbf{2}^{Pd}$.

Figure 7. UV/Vis-spectra of **2** ($c = 2 \cdot 10^{-5}$ M, black) and $\mathbf{2}^{Pd}$ ($c = 5 \cdot 10^{-6}$ M, red) in MeCN, width of cuvette: 10 mm.

As shown in Figure 8, ligand **3** shows strong absorptions between 200 and 330 nm with a local absorption maximum at 321 nm. It displays an extinction coefficient ε_{321} (**3**) = 32500 $l \cdot mol^{-1} \cdot cm^{-1}$. Through coordination to Pd^{II} or Pt^{II} the band shapes alter, resulting in formal hypsochromic shifts of the maxima (313 nm for Pd^{II} and 314 nm for Pt^{II}). The extinction coefficients rise by factors 4.51 and 3.36, respectively to ε_{313} ($\mathbf{3}^{Pd}$) = 146600 $l \cdot mol^{-1} \cdot cm^{-1}$ and ε_{314} ($\mathbf{3}^{Pt}$) = 109300 $l \cdot mol^{-1} \cdot cm^{-1}$, differing +13% and −16% from the expected quadrupling due to the presence of four ligand molecules per cage. Furthermore, upon coordination each a new maximum is observed at 230 nm and 229 nm with extinction coefficients of ε_{230} ($\mathbf{3}^{Pd}$) = 171400 $l \cdot mol^{-1} \cdot cm^{-1}$ and ε_{229} ($\mathbf{3}^{Pt}$) = 142200 $l \cdot mol^{-1} \cdot cm^{-1}$.

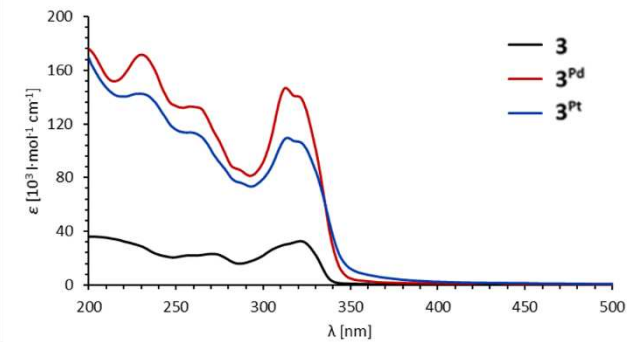

Figure 8. UV/Vis-spectra of **3** ($c = 2 \cdot 10^{-5}$ M, black), $\mathbf{3}^{Pd}$ ($c = 5 \cdot 10^{-6}$ M, red) and $\mathbf{3}^{Pt}$ ($c = 5 \cdot 10^{-6}$ M, blue) in MeCN, width of cuvette: 10 mm.

While absorption properties of **2** and **3** show a minor influence of metal coordination, luminescence is strongly dependent of the metal. Excitation of a solution of **2** in acetonitrile with UV light leads to a strong emission ($\Phi_{290\ nm}$ (**2**) = 42%), with a maximum at $\lambda_{em,max}$ (**2**) = 412 nm. However, coordination to Pd^{II} lowers significantly the quantum yield ($\Phi_{310\ nm}$ ($\mathbf{2}^{Pd}$) = 7%), while the emission maximum remains almost unaffected $\lambda_{em,max}$ ($\mathbf{2}^{Pd}$) = 413 nm, $\Delta\lambda_{em,max}$ = 1 nm), as depicted in Figure 9.

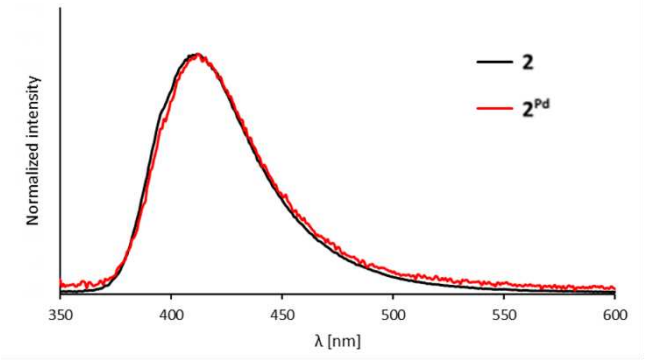

Figure 9. Luminescence spectra of **2** ($2 \cdot 10^{-5}$ M, λ_{ex} = 290 nm) and $\mathbf{2}^{Pd}$ ($5 \cdot 10^{-6}$ M, λ_{ex} = 310 nm) in acetonitrile upon excitation with UV light, intensities normalized.

Ligand **3** shows an even higher quantum yield ($\Phi_{300\ nm}$ (**3**) = 48%), and as intended, the methoxy-functionalization leads to a significantly increased fluorescence compared to the unsubstituted ligand (48% vs. 1.1% Φ).[6a]
Analogous to **2**, upon coordination of Pd^{II}, the quantum yield is lowered significantly to $\Phi_{300\ nm}$ ($\mathbf{3}^{Pd}$) = 3%, the emission maximum is bathochromically shifted from $\lambda_{em,max}$ (**3**) = 345 nm to $\lambda_{em,max}$ ($\mathbf{3}^{Pd}$) = 352 nm. Platinum cage $\mathbf{3}^{Pt}$ is hardly emissive with a quantum yield of less than 0.2%. The emission maximum is almost the same as for $\mathbf{3}^{Pd}$ ($\lambda_{em,max}$ ($\mathbf{3}^{Pd}$) = 349 nm). The emission spectra of all three compounds are shown in Figure 10. Unfortunately, uptake studies of the cages in cells by fluorescence microscopy could not be performed due to low photoluminescence.

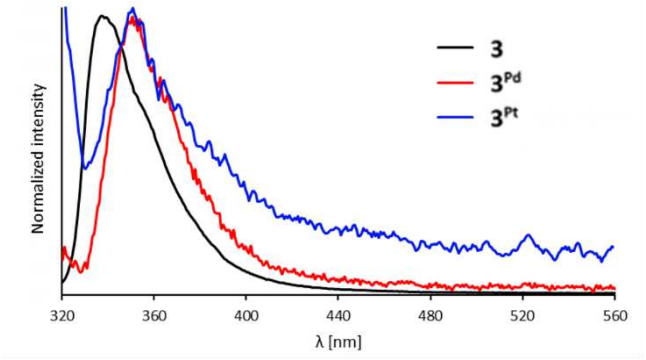

Figure 10. Luminescence spectra in acetonitrile of **3** ($2 \cdot 10^{-5}$ M, λ_{ex} = 300 nm), $\mathbf{3}^{Pd}$ ($5 \cdot 10^{-6}$ M, λ_{ex} = 310 nm) and $\mathbf{3}^{Pt}$ ($5 \cdot 10^{-6}$ M, λ_{ex} = 310 nm) in acetonitrile upon excitation with UV light, intensities normalized.

To examine the encapsulation properties of the palladium cages, solutions of $\mathbf{2}^{Pd}$ and $\mathbf{3}^{Pd}$ were treated with distinct amounts of cisplatin and analyzed by NMR spectroscopy. Convincing evidence for cisplatin encapsulation, both in $\mathbf{2}^{Pd}$ and $\mathbf{3}^{Pd}$ was received. Successive addition of 2 and 10 equivalents of cisplatin in DMF-d_7 to a DMF-d_7 solution of $\mathbf{2}^{Pd}$ results in a significant broadening of the H_e signals. These hydrogen atoms are pointing directly into the cages inner cavity and thus apparently interact with encapsulated cisplatin guest molecules (Figure 11). The other signals remain unaffected. This behavior is consistent with a similar example reported earlier and was described as an indication for the encapsulation of cisplatin.[8a]

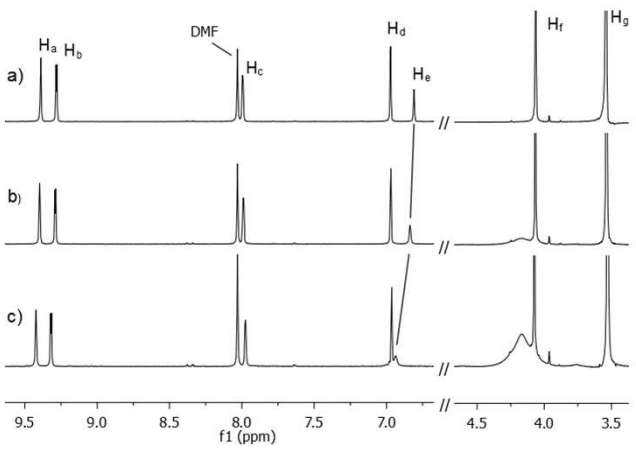

Figure 11. ^{1}H NMR spectrum cutouts (400 MHz, DMF-d_7, 296 K) of: a) $\mathbf{2}^{Pd}$, b) $\mathbf{2}^{Pd}$ with 2 equiv. cisplatin, c) $\mathbf{2}^{Pd}$ with 10 equiv. cisplatin.

Addition of 2 equivalents of cisplatin to a CD_3CN solution of cage $\mathbf{3}^{Pd}$, heating to 60 °C for 10 min and finally ultrasonic treatment for 2 min leads to a distinct, macroscopically visible dissolution of cisplatin. The ^{1}H NMR spectrum gives also evidence for the encapsulation. Primarily the signal from H_a is broadened noticeably and furthermore shifted downfield, thus indicating an interaction with encapsulated guest molecules (Figure 12). This is consistent with similar literature results.[8a, f, g] Alike experiments with $\mathbf{3}^{Pt}$ resulted in decomposition products.

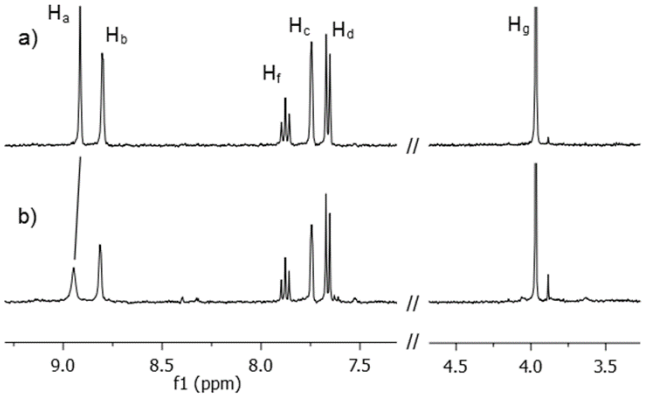

Figure 12. ^{1}H NMR spectrum cutouts (400 MHz, CD_3CN, 296 K) of: a) $\mathbf{3}^{Pd}$, b) $\mathbf{3}^{Pd}$ with 2 equiv. cisplatin.

The palladium cages $\mathbf{2}^{Pd}$ and $\mathbf{3}^{Pd}$ as well as their respective ligands **2** and **3** and the palladium precursor $[Pd(NCCH_3)_4](BF_4)_2$ were screened for their antiproliferative properties in vitro in human cancer cell lines A549 (lung carcinoma) and HepG2 (hepatocellular carcinoma).[18] The IC_{50} (inhibitory concentration to reduce viability to 50%) values of the compounds were determined after 48 hours incubation using the 3-(4,5-dimethylthiazol-2-yl)-2,5-diphenyltetra-zolium bromide (MTT) assay (Table 2). The cage compound $\mathbf{3}^{Pd}$ showed moderate cytotoxicity (IC_{50} = 44-72 µM) in the tested cell lines and is less effective compared to cisplatin, while cage $\mathbf{2}^{Pd}$ is non-cytotoxic. In contrast, the ligands and the Pd precursor are inactive (IC_{50} > 100 µM) in A549 and HepG2.

Table 2. IC_{50} values of the compounds [µM] in A549 and HepG2, [(cisplatin)$_2\subset$ $\mathbf{2}^{Pd}$] and [(cisplatin)$_2\subset$ $\mathbf{3}^{Pd}$], normalized to the concentration of cisplatin.

	IC_{50} [µM] (A549)	IC_{50} [µM] (HepG2)
$[Pd(NCCH_3)_4](BF_4)_2$	> 100	> 100
2	> 100	> 100
3	> 100	96.1 ± 1.4
$\mathbf{2}^{Pd}$	> 100	> 100
$\mathbf{3}^{Pd}$	71.8 ± 9.1	44 ± 11
cisplatin	16.8 ± 0.7	6.7 ± 0.9
[(cisplatin)$_2\subset\mathbf{2}^{Pd}$]	11.0 ± 1.3	5.2 ± 0.3

[(cisplatin)$_2$⊂**3**^{Pd}]	6.6 ± 1.0	13.4 ± 3.0

As previously reported,[8a, g] this type of metallocages can potentially function as drug delivery systems due to their ability to encapsulate two molecules cisplatin. ^{1}H NMR studies provide evidence of the encapsulation of cisplatin within cage **2**^{Pd} and **3**^{Pd} (see Figure 11 and Figure 12). The antiproliferative effects of the host-guest complexes [(cisplatin)$_2$ ⊂ **2**^{Pd}] and [(cisplatin)$_2$ ⊂ **3**^{Pd}] were studied against human carcinoma A549 and HepG2 (Figure 13). Notably, both host-guest systems show an increased cytotoxic effect in A549 compared to cisplatin and the cage by itself, while in HepG2 these systems are similar effective or even less potent than cisplatin. The low cytotoxicity of the cage compounds and the enhanced cytotoxic effect of the host-guest systems compared to cisplatin make these metallocages attractive candidates as drug delivery systems.

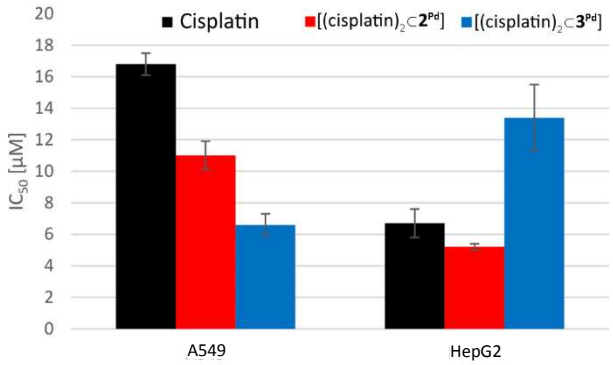

Figure 13 IC_{50} values of Cisplatin and the inclusion compounds [(cisplatin)$_2$ ⊂ **2**^{Pd}] and [(cisplatin)$_2$ ⊂ **3**^{Pd}], normalized to the concentration of cisplatin.

Conclusion

The synthesis and characterization of new M_2L_4 (M = Pd, Pt) molecular cages **2**^{Pd}, **3**^{Pd} and **3**^{Pt}, starting from rigid, highly fluorescent, ligands **2** and **3** is described. The first Pt_2L_4 cage with a rigid *tris*-pyridine ligand (**3**) is presented. Additionally, absorption and photoluminescence studies of both ligands and cages have been performed, showing a lower fluorescence of the metallocages in comparison to the highly fluorescent free ligands. It could be demonstrated that both **2**^{Pd} and **3**^{Pd} are capable of encapsulating the anticancer drug cisplatin. Notably, the palladium precursor and the ligands are non-toxic and the palladium cages possess only a low cytotoxicity in cancer cells. However, the cage compounds encapsulating cisplatin show an increased cytotoxic effect towards human lung cancer cells (A549). Thus, the methoxy-functionalized coordination cages are promising drug delivery vectors for the anticancer agent cisplatin. Further ligand modifications are currently performed in our laboratories to increase cage fluorescence.

Experimental section

General remarks

All chemicals were purchased from commercial sources and used without further purification, solvents were distilled prior to use. NMR-spectra were recorded on a Bruker AV 400 or a Bruker AV 400 HD spectrometer. IR spectra were collected on a Varian 670 spectrometer. ESI HRMS measurements were conducted on a Thermo LTQ FT Ultra. UV/Vis spectra were recorded on an Agilent Cary 60. Emission spectra and absolute quantum yields were obtained on a Hamamatsu Absolute PL QY spectrometer C11347. Compound **1** was synthesized according to literature procedures.[15]

3,5-Bis-((5-methoxypyridin-3-yl)-ethynyl)-aniline (2)

Compound **1** (1.00 g, 7.76 mmol, 4.00 equiv.), 3,5-dibromoaniline (471 mg, 1.88 mmol, 1.00 equiv.), CuI (35.8 mg, 0.19 mmol, 0.10 equiv.) and [$PdCl_2(PPh_3)_2$] (132 mg, 0.19 mmol, 0.10 equiv.) are suspended in degassed NEt_3 (40 ml) and heated to reflux for three days under an argon atmosphere. The suspension is filtered over celite, the filter cake washed with CH_2Cl_2 and the solvent removed under reduced pressure. The crude product is purified by flash chromatography (CH_2Cl_2 : MeOH = 100 : 0 → 96 : 4). The product **2** is obtained as yellow needles (281 mg, 791 µmol, 42%). ^{1}H NMR (400 MHz, CD_3CN, 296 K): δ_H (ppm) = 8.31 (d, ^4J = 1.7 Hz, 2H, H_a), 8.27 (d, ^4J = 2.9 Hz, 2H, H_b), 7.43 (dd, ^4J = 2.9, 1.7 Hz, 2H, H_c), 7.01 (t, ^4J = 1.4 Hz, 1H, H_e), 6.85 (d, ^4J = 1.4 Hz, 2H, H_d), 4.47 (s, 2H, NH_2), 3.87 (s, 6H, H_g). ^{13}C NMR (101 MHz, CD_3CN, 297 K): δ_C (ppm) = 156.2, 149.6, 145.0, 138.7, 124.4, 124.1, 122.9, 121.0, 100.9, 92.3, 86.4, 56.5. DOSY NMR (400 MHz, CD_3CN, 298 K): D ($m^2 \cdot s^{-1}$) = 1.07 · 10^{-9}. HRMS (ESI, MeCN): *m*/*z* = 356.14 [**2**+H]$^+$ (calcd. for $C_{22}H_{18}N_3O_2^+$ 356.14), 178.57 [**2**+2H]$^{2+}$ (calcd. for $C_{22}H_{19}N_3O_2^{2+}$ 178.57). FTIR (KBr): $\tilde{\nu}$ (cm^{-1}) = 3323 (br), 3190 (br), 3072 (w), 2934 (w), 2833 (w), 2211 (w), 1820 (w), 1592 (s), 1454 (m), 1426 (s), 1371 (m), 1314 (m), 1288 (m), 1243 (m), 1213 (s), 1150 (m), 1108 (w), 1055 (s), 1006 (w), 912 (m), 858 (s), 699 (s), 581 (m), 534 (m).

Pd^{II} cage [Pd_2(2)$_4$](BF$_4$)$_4$ (2^{Pd})

A mixture of **2** (32.0 mg, 90.0 µmol, 4.00 eq) and [$Pd(NCCH_3)_4$](BF_4)$_2$ (20.0 mg, 45.0 µmol, 2.00 eq) in 9 ml acetonitrile is heated to reflux for 1 h. After cooling to room temperature, the product is precipitated by addition of diethyl ether (60 ml). The solid is filtered off, washed with diethyl ether and dried under reduced pressure. **2**^{Pd} is obtained as an off-white solid (30.0 mg, 18.2 µmol, 81%). ^{1}H NMR (400 MHz, CD_3CN, 297 K): δ_H (ppm) = 8.90 (d, ^4J = 1.4 Hz, 8H, H_a), 8.79 (d, ^4J = 2.6 Hz, 8H, H_b), 7.64 (dd, ^4J = 2.6, 1.4 Hz, 8H, H_c), 7.18 (t, ^4J = 1.4 Hz, 4H, H_e), 6.88 (d, ^4J = 1.4 Hz, 8H, H_d), 4.57 (s, 8H, NH_2), 3.95 (s, 24H, H_g). ^{13}C NMR (101 MHz, CD_3CN, 293 K): δ_C (ppm) = 158.4, 149.8, 145.6, 139.0, 128.0, 124.6, 124.0, 123.5, 119.2, 95.3, 84.0, 57.7. DOSY NMR (CD_3CN, 400 MHz, 298 K): D ($m^2 \cdot s^{-1}$) = 5.33 · 10^{-10}. HRMS (ESI, MeCN): *m*/*z* = 408.33 [(**2**^{Pd} − 4 BF_4^-)$^{4+}$] (calcd. for $C_{88}H_{68}N_{12}O_8Pd_2^{4+}$ 408.08), 574.11 [(**2**^{Pd} – 3 BF_4^-)$^{3+}$] (calcd. for $C_{88}H_{68}BF_4N_{12}O_8Pd_2^{3+}$ 573.11), 903.67 [(**2**^{Pd} – 2 BF_4^-)$^{2+}$] (calcd. for $C_{88}H_{68}B_2F_8N_{12}O_8Pd_2^{2+}$ 903.17). FTIR (KBr): $\tilde{\nu}$ (cm^{-1}) = 3458 (br), 3387 (br), 3087 (m), 2948 (w), 2220 (m), 1588 (s), 1461 (m), 1427 (m), 1317 (m), 1259 (w), 1222 (m), 1155 (m), 1053 (s), 875 (m), 691 (m), 581 (w), 414 (s).

2,6-Bis-((5-methoxypyridin-3-yl)-ethynyl)-pyridine (3)

3-Ethynyl-5-methoxy pyridine (787 mg, 5.91 mmol, 4.00 eq), 2,6-dibromopyridine (350 mg, 1.48 mmol, 1.00 eq), CuI (28.1 mg, 148 µmol, 0.10 eq) and [$PdCl_2(PPh_3)_2$] (104 mg, 148 µmol, 0.10 eq) are suspended in degassed NEt_3 (27 ml) and heated to reflux for three days under an argon atmosphere. The suspension is filtered over celite, the filter cake washed with CH_2Cl_2 and the solvent removed under reduced pressure. The crude product is purified by flash chromatography (CH_2Cl_2 : MeOH = 99 : 1 → 96 : 4) and product **3** obtained as an off-white solid (420 mg, 1.23 mmol, 83%). ^{1}H NMR (400 MHz, CD_3CN, 296 K): δ_H (ppm) = 8.40 (d, ^4J = 1.6 Hz, 2H, H_a), 8.32 (d, ^4J = 2.9 Hz, 2H, H_b), 7.86 (t, ^3J = 7.8 Hz, 1H, H_f), 7.62 (d, ^3J = 7.8 Hz, 2H, H_d), 7.39 (dd, ^4J = 2.9, 1.6 Hz, 2H, H_c), 3.88 (s, 6H, H_g). ^{13}C NMR (101 MHz, $CDCl_3$, 293 K): δ_C (ppm) = 155.2, 144.9,

143.4, 138.6, 136.9, 126.9, 122.7, 119.5, 90.9, 86.4, 55.8. DOSY NMR (CD_3CN, 400 MHz, 298 K): D ($m^2 \cdot s^{-1}$) = 1.22 · 10^{-9}. HRMS (ESI, MeCN): *m/z* = 342.12 [(**3**+H)$^+$] (calcd. for $C_{21}H_{16}N_3O_2^+$ 342.12), 171.57 [(**3**+2H)$^{2+}$] (calcd. for $C_{21}H_{17}N_3O_2^{2+}$ 171.57). FTIR (KBr): $\tilde{\nu}$ (cm^{-1}) = 3438 (br), 3046 (w), 2983 (w), 2946 (w), 2219 (w), 1582 (s), 1454 (s), 1417 (s), 1313 (w), 1256 (s), 1223 (s), 1166 (m), 1038 (s), 1013 (m), 947 (m), 908 (w), 875 (m), 805 (m), 747 (w), 700 (m), 671 (m), 585 (w), 545 (m), 410 (s).

Pd^{II} cage $[Pd_2(3)_4](BF_4)_4$ (3^{Pd})

A mixture of **3** (14.3 mg, 41.9 µmol, 4.00 eq) and $[Pd(NCCH_3)_4](BF_4)_2$ (9.30 mg, 21.0 µmol, 2.00 eq) in 10 ml MeCN is heated to reflux for 1 h and the product precipitated by addition of diethyl ether (80 ml) after cooling to 4 °C. The solid is centrifuged off, washed with diethyl ether (10 ml) and dried *in vacuo*. $\mathbf{3^{Pd}}$ is obtained as an off-white solid (20.2 mg, 10.5 µmol, 100%). ^{1}H NMR (400 MHz, CD_3CN, 297 K): δ_H (ppm) = 8.92 (d, ^4J = 1.4 Hz, 8H, H_a), 8.82 (d, ^4J = 2.6 Hz, 8H, H_b), 7.88 (dd, ^4J = 8.2, 7.5 Hz, 4H, H_f), 7.74 (dd, ^4J = 2.6, 1.4 Hz, 8H, H_c), 7.66 (d, ^4J = 7.8 Hz, 8H, H_d), 3.97 (s, 24H, H_g). ^{13}C NMR (101 MHz, CD_3CN, 297 K): δ_C (ppm) = 158.5, 146.0, 143.3, 139.8, 138.7, 129.4, 128.7, 123.7, 94.1, 83.3, 57.8. DOSY NMR (CD_3CN, 400 MHz, 298 K): D ($m^2 \cdot s^{-1}$) = 5.58 · 10^{-10}. HRMS (ESI, MeCN): *m/z* = 394.32 [($\mathbf{3^{Pd}}$ − 4 BF_4^-)$^{4+}$] (calcd. for $C_{84}H_{60}N_{12}O_8Pd_2^{4+}$ 394.07), 555.43 [($\mathbf{3^{Pd}}$ − 3 BF_4^-)$^{3+}$] (calcd. for $C_{84}H_{60}BF_4N_{12}O_8Pd_2^{3+}$ 554.42), 874.64 [($\mathbf{3^{Pd}}$ − 2 BF_4^-)$^{2+}$] (calcd. for $C_{84}H_{60}B_2F_8N_{12}O_8Pd_2^{2+}$ 875.14). FTIR (KBr): $\tilde{\nu}$ (cm^{-1}) = 3430 (br), 3088 (m), 2947 (w), 2850 (w), 2224 (w), 1813 (w), 1587 (s), 1456 (s), 1336 (s), 1248 (s), 1150 (s), 1055 (s), 876 (m), 809 (m), 731 (w), 691 (m), 589 (w), 532 (w), 419 (w).

Pt^{II} cage $[Pt_2(3)_4](ClO_4)_4$ (3^{Pt})

A mixture of **3** (25.4 mg, 74.3 µmol, 4.00 eq), $[PtCl_2(NCCH_3)_2]$ (12.9 mg, 37.1 µmol, 2.00 eq) and $AgClO_4$ (15.4 mg, 74.3 µmol, 4.00 eq) is dispersed in 3 ml acetonitrile and heated to reflux for 2 days in the dark. The dispersion is filtered, the product precipitated by addition of diethyl ether (30 ml) and centrifuged. The crude product is dissolved in acetonitrile, filtered over silica and the silica washed with acetonitrile (20 ml). The product is eluted from silica with a mixture of acetone : methanol : water : $KNO_{3(aq)}$ (sat.) = 24 : 12 : 3 : 1. The organic solvents are evaporated under reduced pressure, the solid centrifuged off, dissolved in acetonitrile and filtered. After addition of 1 mL sat. aqueous $LiClO_4$ the organic solvents are evaporated under reduced pressure, the product centrifuged off the resulting dispersion, washed with water (2 × 10 ml), ethanol (2 ml) and diethyl ether (10 mL) and dried *in vacuo*. $\mathbf{3^{Pt}}$ is obtained as a pale brown solid (8.00 mg, 3.72 µmol, 20%). ^{1}H NMR (400 MHz, CD_3CN, 296 K): δ_H (ppm) = 8.87 (d, ^4J = 1.5 Hz, 8H, H_a), 8.84 (d, ^4J = 2.6 Hz, 8H, H_b), 7.88 (dd, ^3J = 8.2, 7.4 Hz, 4H, H_f), 7.73 (dd, ^4J = 2.6, 1.5, 8H, H_c), 7.67 (d, ^3J = 7.8 Hz, 8H, H_d), 3.98 (s, 24H, H_g). ^{13}C NMR (101 MHz, CD_3CN, 293 K): δ_C (ppm) = 158.8, 147.0, 143.3, 140.9, 138.7, 129.4, 129.1, 123.9, 94.0, 83.1, 58.0. DOSY NMR (CD_3CN, 400 MHz, 298 K): D ($m^2 \cdot s^{-1}$) = 5.60 · 10^{-10}. HRMS (ESI, MeCN): *m/z* = 438.60 [($\mathbf{3^{Pt}}$ − 4 ClO_4^-)$^{4+}$] (calcd. for $C_{84}H_{60}N_{12}O_8Pt_2^{4+}$ 438.60), 618.11 [($\mathbf{3^{Pt}}$ − 3 ClO_4^-)$^{3+}$] (calcd. for $C_{84}H_{60}ClN_{12}O_{12}Pt_2^{3+}$ 618.11), 977.15 [($\mathbf{3^{Pt}}$ − 2 ClO_4^-)$^{2+}$] (calcd. for $C_{84}H_{60}Cl_2N_{12}O_{16}Pt_2^{2+}$ 977.15). FTIR (ATR): $\tilde{\nu}$ (cm^{-1}) = 3084 (w), 2158 (w), 1585 (m), 1456 (m), 1425 (w), 1334 (w), 1315 (w), 1248 (w), 1234 (w), 1092 (vs), 1014 (w), 984 (w), 876 (m), 810 (w), 690 (m), 623 (s).

MTT cytotoxicity assay standard procedure:

This essay was performed in 96 well plates. A549/HepG2 cells were grown to 30-40 % confluence. The medium was removed and 100 µL medium /well containing 1 µL DMF compound stock were added to the cells and incubated for 48 h. All concentrations as well as a DMF control were tested in technical triplicates and biological duplicates. 20 µL Thiazolyl Blue Tetrazolium bromide (5 mg/mL in PBS, Sigma Aldrich) were added to the cells and incubated for 2-4 h until complete consumption was observed. After removal of the medium, the resulting formazan was dissolved in 200 µL DMSO. Optical density was measured at 570 nm (562 nm) and background subtracted at 630 nm (620 nm) by a TECAN Infinite® M200 Pro. For calculation of IC_{50} values, residual viabilities for the respective compound concentration were fitted to viability [%], inhibitor concentration [µM] and Hill slope using Graphpad Prism 6.0.

Crystallographic details

Additional details of the crystallographic measurements can be found in the Supporting Information. CCDC numbers: 1453095-1453096.

Acknowledgement

Supported by Deutsche Forschungsgemeinschaft (DFG) through the TUM International Graduate School of Science and Engineering (IGSSE). The authors are grateful for the financial support of the TUM Graduate School of Chemistry. EU COST action CM1105 is gratefully acknowledged for funding and fruitful discussion. Dr. Alexander Pöthig is acknowledged for crystallographic advice and assistance with the photoluminescence measurements.

Keywords

Drug delivery, antitumor agents, cisplatin, coordination cages, self-assembly

References and notes

[1] D. A. McMorran and P. J. Steel, *Angew. Chem. Int. Ed.* **1998**, *37*, 3295-3297.

[2] a) A. Schmidt, A. Casini and F. E. Kühn, *Coord. Chem. Rev.* **2014**, *275*, 19-36; b) M. Han, D. M. Engelhard and G. H. Clever, *Chem. Soc. Rev.* **2014**, *43*, 1848-1860; c) N. B. Debata, D. Tripathy and D. K. Chand, *Coord. Chem. Rev.* **2012**, *256*, 1831-1945.

[3] a) Z. Li, N. Kishi, K. Yoza, M. Akita and M. Yoshizawa, *Chem. Eur. J.* **2012**, *18*, 8358-8365; b) C. Desmarets, T. Ducarre, M. Rager, G. Gontard and H. Amouri, *Materials* **2014**, *7*, 287-301.

[4] a) H. Amouri, C. Desmarets, A. Bettoschi, M. N. Rager, K. Boubekeur, P. Rabu and M. Drillon, *Chem. Eur. J.* **2007**, *13*, 5401-5407; b) H. Amouri, L. Mimassi, M. N. Rager, B. E. Mann, C. Guyard-Duhayon and L. Raehm, *Angew. Chem. Int. Ed. Engl.* **2005**, *44*, 4543-4546; c) C. Desmarets, F. Poli, X. F. Le Goff, K. Muller and H. Amouri, *Dalton Trans.* **2009**, 10429-10432; d) B. Wu, D. Yuan, B. Lou, L. Han, C. Liu, C. Zhang and M. Hong, *Inorg. Chem.* **2005**, *44*, 9175-9184; e) Y.-B. Xie, J.-R. Li, C. Zhang and X.-H. Bu, *Cryst. Growth Des.* **2005**, *5*, 1743-1749.

[5] a) C. Desmarets, C. Policar, L.-M. Chamoreau and H. Amouri, *Eur. J. Inorg. Chem.* **2009**, *2009*, 4396-4400; b) H.-K. Liu, Y. Cai, W. Luo, F. Tong, C. You, S. Lü, X. Huang, H.-Y. Ye, F. Su and X. Wang, *Inorg. Chem. Commun.* **2009**, *12*, 457-460.

[6] a) A. M. Johnson, O. Moshe, A. S. Gamboa, B. W. Langloss, J. F. Limtiaco, C. K. Larive and R. J. Hooley, *Inorg. Chem.* **2011**, *50*, 9430-9442; b) J. E. M. Lewis, A. B. S. Elliott, C. J. McAdam, K. C. Gordon and J. D. Crowley, *Chem. Sci.* **2014**, *5*, 1833-1843; c) Z. Li, N. Kishi, K. Hasegawa, M. Akita and M. Yoshizawa, *Chem. Commun.* **2011**, *47*, 8605-8607; d) M. Yamashina, M. M. Sartin, Y. Sei, M. Akita, S. Takeuchi, T. Tahara and M. Yoshizawa, *J. Am. Chem. Soc.* **2015**, *137*, 9266-9269; e) A. Schmidt, M. Hollering, M. Drees, A. Casini and F. E.

Kühn, *Dalton Trans.* **2016**, *45*, 8556-8565; f) A. B. Elliott, J. E. Lewis, H. van der Salm, C. J. McAdam, J. D. Crowley and K. C. Gordon, *Inorg. Chem.* **2016**, *55*, 3440-3447.

[7] a) D. K. Chand, K. Biradha and M. Fujita, *Chem. Commun.* **2001**, 1652-1653; b) D. K. Chand, M. Fujita, K. Biradha, S. Sakamoto and K. Yamaguchi, *Dalton Trans.* **2003**, 2750-2756.

[8] a) A. Schmidt, V. Molano, M. Hollering, A. Pöthig, A. Casini and F. E. Kühn, *Chem. Eur. J.* **2016**, *22*, 2253-2256; b) B. Therrien, G. Suss-Fink, P. Govindaswamy, A. K. Renfrew and P. J. Dyson, *Angew. Chem. Int. Ed. Engl.* **2008**, *47*, 3773-3776; c) Y. R. Zheng, K. Suntharalingam, T. C. Johnstone and S. J. Lippard, *Chem. Sci.* **2015**, *6*, 1189-1193; d) J. Mattsson, O. Zava, A. K. Renfrew, Y. Sei, K. Yamaguchi, P. J. Dyson and B. Therrien, *Dalton Trans.* **2010**, *39*, 8248-8255; e) N. P. Barry, O. Zava, P. J. Dyson and B. Therrien, *Chem. Eur. J.* **2011**, *17*, 9669-9677; f) J. E. Lewis, C. J. McAdam, M. G. Gardiner and J. D. Crowley, *Chem. Commun.* **2013**, *49*, 3398-3400; g) J. E. M. Lewis, E. L. Gavey, S. A. Cameron and J. D. Crowley, *Chem. Sci.* **2012**, *3*, 778-784.

[9] a) A. Ahmedova, D. Momekova, M. Yamashina, P. Shestakova, G. Momekov, M. Akita and M. Yoshizawa, *Chem. Asian J.* **2016**, *11*, 474-477; b) D. Preston, S. M. McNeill, J. E. Lewis, G. I. Giles and J. D. Crowley, *Dalton Trans.* **2016**, *45*, 8050-8060; c) A. Ahmedova, R. Mihaylova, D. Momekova, P. Shestakova, S. Stoykova, J. Zaharieva, M. Yamashina, G. Momekov, M. Akita and M. Yoshizawa, *Dalton Trans.* **2016**, *45*, 13214-13221.

[10] a) M. G. Apps, E. H. Choi and N. J. Wheate, *Endocr. Relat. Cancer* **2015**, *22*, R219-R233; b) N. J. Wheate, S. Walker, G. E. Craig and R. Oun, *Dalton Trans.* **2010**, *39*, 8113-8127.

[11] Y. Matsumura and H. Maeda, *Cancer Res.* **1986**, *46*, 6387-6392.

[12] a) J. M. Meerum Terwogt, G. Groenewegen, D. Pluim, M. Maliepaard, M. M. Tibben, A. Huisman, W. W. ten Bokkel Huinink, M. Schot, H. Welbank, E. E. Voest, J. H. Beijnen and J. M. Schellens, *Cancer Chemother. Pharmacol.* **2002**, *49*, 201-210; b) M. S. Newman, G. T. Colbern, P. K. Working, C. Engbers and M. A. Amantea, *Cancer Chemother. Pharmacol.* **1999**, *43*, 1-7; c) V. Chupin, A. I. de Kroon and B. de Kruijff, *J. Am. Chem. Soc.* **2004**, *126*, 13816-13821; d) S. Khiati, D. Luvino, K. Oumzil, B. Chauffert, M. Camplo and P. Barthelemy, *ACS Nano* **2011**, *5*, 8649-8655; e) S. C. White, P. Lorigan, G. P. Margison, J. M. Margison, F. Martin, N. Thatcher, H. Anderson and M. Ranson, *Br. J. Cancer* **2006**, *95*, 822-828.

[13] a) S. D. Brown, P. Nativo, J.-A. Smith, D. Stirling, P. R. Edwards, B. Venugopal, D. J. Flint, J. A. Plumb, D. Graham and N. J. Wheate, *J. Am. Chem. Soc.* **2010**, *132*, 4678-4684; b) S. Dhar, W. L. Daniel, D. A. Giljohann, C. A. Mirkin and S. J. Lippard, *J. Am. Chem. Soc.* **2009**, *131*, 14652-14653.

[14] a) A. M. Krause-Heuer, N. J. Wheate, M. J. Tilby, D. G. Pearson, C. J. Ottley and J. R. Aldrich-Wright, *Inorg. Chem.* **2008**, *47*, 6880-6888; b) N. J. Wheate, D. P. Buck, A. I. Day and J. G. Collins, *Dalton Trans.* **2006**, 451-458; c) N. J. Wheate, A. I. Day, R. J. Blanch, A. P. Arnold, C. Cullinane and J. Grant Collins, *Chem. Commun.* **2004**, 1424-1425; d) N. J. Wheate, R. I. Taleb, A. M. Krause-Heuer, R. L. Cook, S. Wang, V. J. Higgins and J. R. Aldrich-Wright, *Dalton Trans.* **2007**, 5055-5064.

[15] C. B. Aakeröy, N. Schultheiss and J. Desper, *Inorg. Chem.* **2005**, *44*, 4983-4991.

[16] a) J. T. Edward, *J. Chem. Educ.* **1970**, *47*, 261-270; b) A. Einstein, *Ann. Phys.* **1905**, *322*, 549-560.

[17] a) N. Kishi, Z. Li, K. Yoza, M. Akita and M. Yoshizawa, *J. Am. Chem. Soc.* **2011**, *133*, 11438-11441; b) G. H. Clever, W. Kawamura and M. Shionoya, *Inorg. Chem.* **2011**, *50*, 4689-4691; c) G. H. Clever, S. Tashiro and M. Shionoya, *J. Am. Chem. Soc.* **2010**, *132*, 9973-9975; d) G. H. Clever and M. Shionoya, *Chem. Eur. J.* **2010**, *16*, 11792-11796; e) G. H. Clever, S. Tashiro and M. Shionoya, *Angew. Chem. Int. Ed.* **2009**, *48*, 7010-7012; f) M. Fukuda, R. Sekiya and R. Kuroda, *Angew. Chem. Int. Ed.* **2008**, *47*, 706-710; g) N. L. S. Yue, D. J. Eisler, M. C. Jennings and R. J. Puddephatt, *Inorg. Chem.* **2004**, *43*, 7671-7681; h) P. Liao, B. W. Langloss, A. M. Johnson, E. R. Knudsen, F. S. Tham, R. R. Julian and R. J. Hooley, *Chem. Commun.* **2010**, *46*, 4932-4934; i) A. M. Johnson and R. J. Hooley, *Inorg. Chem.* **2011**, *50*, 4671-4673.

[18] as mentioned before, $\mathbf{3^{Pt}}$ was not examined due to the instability towards oxygen and possible instability in the presence of cisplatin.

FULL PAPER

New non-toxic, self-assembled M_2L_4 coordination cages are synthesized from highly fluorescent ligands. The cages are able to encapsulate the anticancer drug cisplatin and enhance its cytotoxicity towards cancer cells.

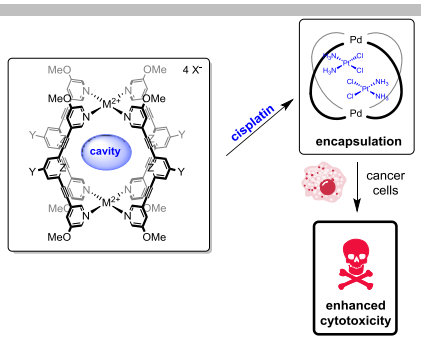

*Felix Kaiser, Andrea Schmidt, Wolfgang Heydenreuter, Philipp J. Altmann, Angela Casini, Stephan A. Sieber and Fritz E. Kühn**

Page No. – Page No.

Self-assembled palladium and platinum coordination cages: Photophysical studies and anticancer activity

Key topic: coordination cages